Validation of stratospheric temperatures measured by Michelson Interferometer for Passive Atmospheric Sounding (MIPAS) on Envisat

D. Y. Wang,[1,2] T. von Clarmann,[1] H. Fischer,[1] B. Funke,[3] S. Gil-López,[3] N. Glatthor,[1] U. Grabowski,[1] M. Höpfner,[1] M. Kaufmann,[3,4] S. Kellmann,[1] M. Kiefer,[1] M. E. Koukouli,[3] A. Linden,[1] M. López-Puertas,[3] G. Mengistu Tsidu,[1] M. Milz,[1] T. Steck,[1] G. P. Stiller,[1] A. J. Simmons,[5] A. Dethof,[5] R. Swinbank,[6] C. Marquardt,[6] J. H. Jiang,[7] L. J. Romans,[7] J. Wickert,[8] T. Schmidt,[8] J. Russell III,[9] and E. Remsberg[10]

Received 12 August 2004; revised 30 November 2004; accepted 13 January 2005; published 20 April 2005.

[1] The Michelson Interferometer for Passive Atmospheric Sounding (MIPAS) onboard the Envisat satellite provides temperature and various gas profiles from limb-viewing midinfrared emission measurements. The stratospheric temperatures retrieved at the Institut für Meteorologie und Klimaforschung (IMK) for September/October 2002 and October/November 2003 are compared with a number of reference data sets, including global radiosonde (RS) observations, radio occultation (RO) measurements of Global Positioning System (GPS) on German Challenging Minisatellite Payload (CHAMP) and Argentinean Satelite de Aplicaciones Cientificas-C (SAC-C) satellite, Halogen Occultation Experiment (HALOE) on the Upper Atmosphere Research Satellite (UARS), and the analyses of European Centre for Medium-Range Weather Forecasts (ECMWF) and Met Office (METO), United Kingdom. The data sets show a good general agreement. Between 10 and 30 km altitude the mean differences are within ±0.5 K for the averages over the height interval and within ±(1–1.5) K at individual levels for comparisons with RS, GPS-RO/CHAMP, and SAC-C, ECMWF, and METO. Between 30 and 45 km the MIPAS mean temperatures, averaged over the height region, are higher than ECMWF but lower than METO by ∼1.5 K, while they differ by ±0.5 K with respect to HALOE, with maximum discrepancies of ∼2.5 K peaking around 35 km. Between 45 and 50 km, MIPAS temperatures show a low bias compared to HALOE, ECMWF, and METO with mean differences of −1 to −3 K and with a better agreement with HALOE. The large discrepancies between MIPAS and the analyses above 30 km likely suggest deficiency in the underlying general circulation models. The standard deviations vary between 2.5 and 3.5 K for individual data sets, with more than 70% being contributed from the expected variability of the atmosphere. Retrieved temperatures with accuracy of ∼0.5–1 K after removing the atmospheric variability provide highly accurate knowledge to characterize our environment.

Citation: Wang, D. Y., et al. (2005), Validation of stratospheric temperatures measured by Michelson Interferometer for Passive Atmospheric Sounding (MIPAS) on Envisat, *J. Geophys. Res.*, *110*, D08301, doi:10.1029/2004JD005342.

1. Introduction

[2] The Michelson Interferometer for Passive Atmospheric Sounding (MIPAS) [*Fischer and Oelhaf*, 1996; *European Space Agency*, 2000] onboard the Envisat satellite is a high-

[1]Institut für Meteorologie und Klimaforschung (IMK), Forschungszentrum Karlsruhe GmbH und Universität Karlsruhe, Karlsruhe, Germany.
[2]Now at Science Application International Corporation/General Science Operation, MODIS Characterization Support Team, Seabrook, Maryland, USA.
[3]Instituto de Astrofísica de Andalucía, Consejo Superior de Investigaciones Científicas, Granada, Spain.
[4]Now at Research Center Juelich (ICG-I), Juelich, Germany.
[5]European Centre for Medium-Range Weather Forecasts, Reading, UK.
[6]Met Office, Exeter, UK.
[7]Jet Propulsion Laboratory, California Institute of Technology, Pasadena, California, USA.
[8]Department 1, Geodesy and Remote Sensing, GeoForschungsZentrum Potsdam (GFZ), Potsdam, Germany.
[9]Department of Physics, Hampton University, Hampton, Virginia, USA.
[10]Atmospheric Sciences Competency, NASA Langley Research Center, Hampton, Virginia, USA.

0148-0227/05/2004JD005342$09.00

Table 1. Numbers of Correlative Profiles Used for Temperature Comparison: Data From Assimilation Analyses, Other Satellite Measurements, and Worldwide Radiosonde (RS) Observations[a]

Time	ECMWF	METO	CHAMP (GFZ)	CHAMP (JPL)	SAC-C	HALOE	RS
18–28 Sept. 2002	4,152	488	902/1060	716/810	880/1005	122/123	94/200
11–13 Oct. 2002	1,090	86	233/260	207/232	225/294	5	361/942
21–31 Oct. 2003	5,111	654	1045/1116	906/968		54	302/717
1–12 Nov. 2003	4,411	612/613	972/1037	805/869		180	367/804
Total	14,744	1840/1841	3152/3473	2634/2879	1135/1299	361/362	757/1859

[a]See the text for coincidence criteria. The numbers of available MIPAS measurements are equal to those of coincidence events for ECMWF data, which are used as initial guess for the IMK-IAA retrievals. For other data sets, one MIPAS profile may have multiple coincidences. This is indicated by paired numbers with the first for MIPAS and the second for the correlative measurements.

resolution Fourier transform spectrometer. It measures vertical profiles of temperature and volume mixing ratio (VMR) of various gas species in the troposphere and stratosphere by limb-observing midinfrared emissions. Complementary to the ESA operational data products [*Carli et al.*, 2004], there are six different off-line data processors at five institutions for science-oriented data analysis of the high-resolution limb-viewing infrared spectra [*von Clarmann et al.*, 2003a].

[3] Since middle infrared emission spectra are strongly sensitive to temperature, and as limb observations are strongly affected by the observation geometry, an accurate knowledge of these quantities is an essential. The data processor developed at Institut für Meteorologie und Klimaforschung (IMK) and complemented by the component of nonlocal thermodynamic equilibrium (non-LTE) treatment from the Instituto de Astrofísica de Andalucía (IAA) provides simultaneous retrieval of temperature and line-of-sight parameters from measured spectra and the spacecraft ephemerides [*von Clarmann et al.*, 2003b]. In this scheme, each single tangent altitude is formally retrieved as an absolute quantity, while information on the relative tangent altitudes, i.e., vertical distances between adjacent tangent altitudes, are retrieved implicitly. A hydrostatic pressure profile is then calculated by using the pressure at one altitude from European Centre for Medium-Range Weather Forecasts (ECMWF) data [e.g., *Simmons et al.*, 2005]. The details of the applied retrieval scheme and its robustness and accuracy have been discussed by *von Clarmann et al.* [2003a, 2003b, 2003c], *Stiller et al.* [2003], and *Steck* [2003]. The MIPAS IMK-IAA temperatures have been compared with a number of other satellite measurements. The preliminary results show good agreement [*Wang et al.*, 2004a, 2004b, 2004c; *Jiang et al.*, 2004; *Dethof et al.*, 2004].

[4] In this study, the IMK-IAA MIPAS temperatures are compared with (1) assimilation analyses of the ECMWF and the Met Office, UK (METO, also previously referred to as UKMO) [*Swinbank and O'Neill*, 1994; *Swinbank et al.*, 2002]; (2) worldwide radiosonde (RS) measurements; (3) radio occultation (RO) measurements of Global Positioning System (GPS) on German Challenging Minisatellite Payload (CHAMP) and Argentinean Satelite de Aplicaciones Cientificas-C (SAC-C) satellites [*Hajj et al.*, 2002, 2004; *Wickert et al.*, 2004a, 2004b]; and (4) solar occultation observations of Halogen Occultation Experiment (HALOE) on the Upper Atmosphere Research Satellite (UARS) [*Russell et al.*, 1993; *Remsberg et al.*, 2002]. The data characteristics and our comparison method are described in sections 2 and 3 respectively. The comparison results are exhibited in section 4. Our conclusions are contained in section 5.

2. Data Description

2.1. IMK-IAA MIPAS Data

[5] The MIPAS temperatures to be validated are the IMK-IAA retrievals. A total of ~15,000 profiles are used for this analysis (see Table 1). They are taken from 14 days in September/October of 2002 (version V1_T + LOS-H_1, previously referred to as version 1.0 by *Wang et al.* [2004a, 2004b, 2004c]) and 20 days in October/November of 2003 (version V2_T+LOS-H_3), and will be referred to as periods I and II, respectively. The MIPAS observations provide global coverage with 14.4 orbits per day. The standard observation mode covers nominal tangent altitudes between 6 and 42 km at a step width of ~3 km, then 47, 52, 60, and 68 km. The spatial sampling interval is ~500 km along-track and ~2800 km across-track at the equator. Some measurements are rejected due to severe cloud contamination (see *Spang et al.* [2004] for details of the cloud-clearing technique). The number of available measurements for each day varies from several tens to hundreds, and the altitude coverage also slightly changes from profile to profile. The IMK-IAA temperatures are derived from infrared emissions based on the operational ESA level 1B data (i.e., calibrated and geolocated radiance spectra). The retrieval is performed between 6 and 70 km on a fixed 1-km grid below 44 km and 2-km grid above, with temperature and tangent altitudes retrieved simultaneously.

[6] Because of the rapid evolution of MIPAS data processing, different ESA level 1B data versions V4.53 and V4.59 are used for the IMK-IAA retrievals of periods I and II. One of the important changes in the two versions is the instrument pointing information. The ESA pointing data are based on the satellite's orbit and attitude control system which uses star tracker information as a reference. These data are henceforth called engineering or initial data (used as initial guess in the IMK-IAA retrievals). In the V4.53 engineering data, both systematic and periodic pointing calibration errors, as well as occasional pitch jumps were detected [*von Clarmann et al.*, 2003b]. In the V4.59 data, a bias as well as harmonic correction has been applied to the nominal pointing calibration. The pointing errors have been corrected to a major part. As shown in Figure 1, the differences between IMK-IAA retrieved and the initial

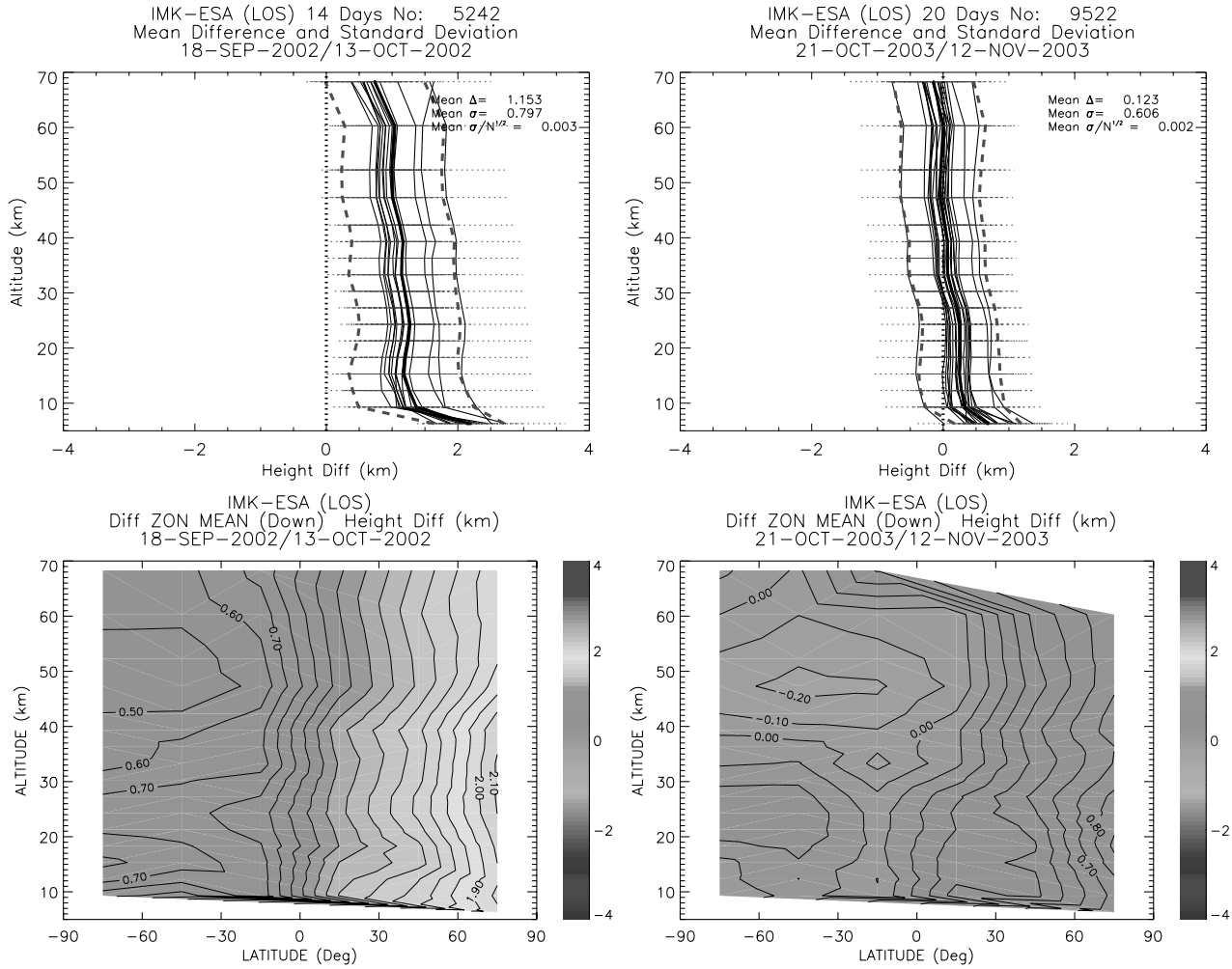

Figure 1. Differences between the IMK-retrieved and ESA-provided nominal MIPAS tangent altitudes (in km). The IMK minus ESA residuals are calculated from the available measurements (see Table 1). The data are averaged over the 14 days in (left) period I and (right) 20 days in period II. The zonal mean differences are derived with a latitude interval of 30° for the MIPAS descending (daytime, bottom plots) orbit node. The contour intervals are 0.1 km. On the top plots, the global means (solid) and standard deviations (dashed) are computed for each day (thin line) and for all days (thick line) of the observations. The total number of profiles are specified in the headings. Also denoted are the global mean difference Δ, standard deviations σ, and the 1-σ error $\sigma/\sqrt{N}$ averaged over all heights, where N is total number of available data points. See color version of this figure in the HTML.

tangent altitudes averaged over all available data points are as large as ~1.15 km for period I but only ~0.12 km for period II, with root-mean-square (rms) deviations of ~0.8 km and 0.6 km, respectively. The discrepancies between the retrieved and initial tangent altitudes show maximum values in the northern polar region, as large as 2 km for period I but only 0.7 km for period II. The differences between the retrieved and initial tangent altitudes also show considerable day-to-day variations but little height variations above 10 km. However, since retrieval of IMK MIPAS temperatures assessed in this paper does not rely on the engineering tangent altitudes, the related change in ESA pointing data processing is not relevant to intercomparison of IMK MIPAS temperatures to the data from other sources.

[7] Another important difference is that the information of the instrumental line shape (ILS) was insufficient for period I but greatly improved for period II. The corrected ILS data used in IMK-IAA retrievals of period II (F. Hase, personal communication, 2003) resemble the latest ESA results. They are constant (as should be expected from instrumental parameters of misalignment), not a function of wave number, and self-consistent in a sense that we can guarantee that the same ILS model has been used within the radiative transfer model. A linear error assessment has been carried out by using the corrected ILS parameters to estimate the effects of ILS bias in version V4.53 on the IMK-IAA retrievals of period I [*Wang et al.*, 2004c]. The ILS error is of systematic nature and is not removed when further averaging the MIPAS total error for a large ensemble. For an average of one orbit, the mean temperatures of period I are likely to be underestimated by ~0.5 K around 20 and 50 km, where the ILS bias is the major contribution to the total error budget, and by ~0.2 K around 40 km, but slightly overestimated by less than ~0.2 K near 30 km.

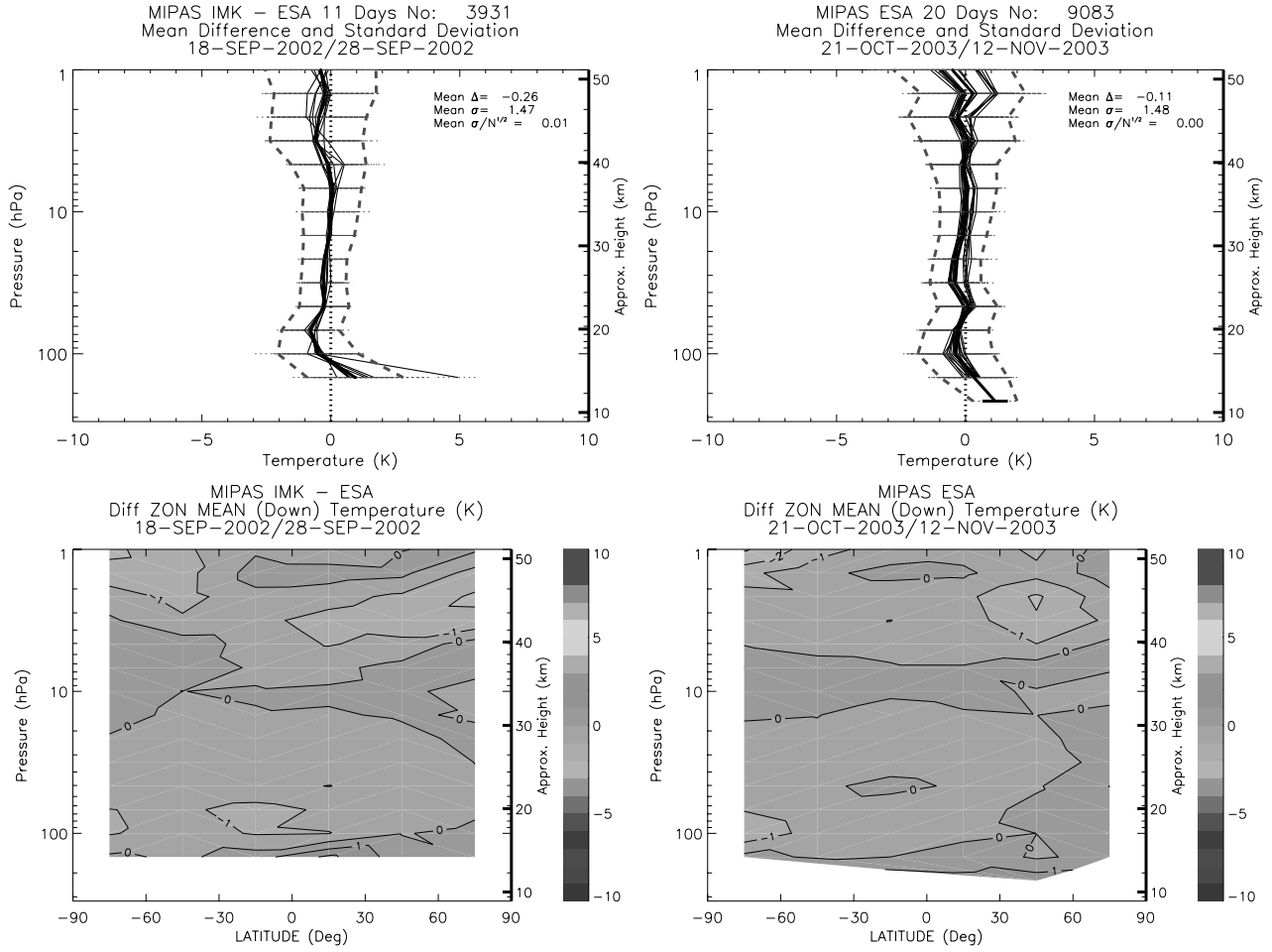

Figure 2. Same as Figure 1, but for comparison between IMK-retrieved and ESA operational MIPAS temperatures. For period I the ESA operational level 2 data are available only for 11 days in September 2002. See color version of this figure in the HTML.

[8] It is also worth noting that the original CO_2 lines of the 1996 High-Resolution Transmission (HITRAN) database [*Rothman et al.*, 1998] were used for modeling CO_2 signatures in MIPAS/Envisat spectra and for the retrieval of temperature and instrumental line of sight (LOS) in the IMK-IAA algorithm until May 2004. Since then the CO_2 line data were updated for the four most abundant isotopic variants of CO_2 (C. Piccolo, personal communication, 2002). The effect of this update on the retrievals was investigated. At altitudes of 10 and 50 km, the differences between temperatures retrieved with the new and the HITRAN96 CO_2 line data set are generally within ±0.2 K. These temperature differences are correlated with differences of less than 100 meters in the retrieved tangent heights.

[9] For cross check, the IMK-IAA MIPAS temperatures are compared with the ESA operational data based on the same level 1B version. Comparison with the ESA data of the most recent version V4.61 is given by *Dethof et al.* [2004]. The ESA operational temperature profiles are retrieved with a vertical resolution of ∼3 km and with the altitudes registered by the engineering measurements. To avoid the influence of the error in the ESA MIPAS altitude registration, the comparisons are conducted in pressure coordinates. The ESA operational level 2 data are available only for 11 days of September 2002. The global and zonal mean differences between the two data sets are displayed in Figure 2. The MIPAS ESA and IMK-IAA temperatures generally show good consistency. The mean differences averaged over the altitude region between 200 and 1 hPa are only −0.3 and −0.1 K in periods I and II, respectively, with a standard deviation of ∼1.5 K. The ESA temperatures are slightly higher than the IMK-IAA data.

2.2. Correlative Data

[10] The correlative data sets used for comparison with the IMK-IAA MIPAS temperatures are described as follows. The temperatures of the ECMWF analyses are stored in spectral form. They are available every 6 hours on standard pressure levels from the ground to 0.1 hPa (at levels of 1013.25, 1000, 850, 700, 500, 300, 200, 140, 100, 90, 70, 50, 30, 20, 14, 10, 7, 5, 3, 2, 1.4, 1, 0.7, 0.5, 0.3, 0.2, 0.14, and 0.1 hPa) and on a regular 1.25° × 1.25° longitude-latitude grid. The temperature data are interpolated onto the altitude, latitude, longitude, and universal time (UT) of the corresponding MIPAS measurements, and are used as a priori information in the IMK-IAA retrievals.

[11] The METO data are available daily at 12:00 UTC on a global grid of 2.5° latitude by 3.75° longitude at the 22 standard UARS pressure levels from 1000 hPa to

0.316 hPa inclusive (0 to 55 km approximately), i.e., $1000 \times 10^{-i/6}$, with i = 0 to 21. The assimilation system that produces the Met Office stratospheric data has been changed to use the New Dynamics (ND) version of the Unified Model since 28 October 2003, and three additional levels are output (25 instead of 22), up to 0.1 hPa (instead of 0.316 hPa).

[12] The global radiosonde stations conduct ascents up to four times daily at the synoptic hours of 00, 06, 12, 18 GMT. The data comprise vertical profiles of temperature between the Earth's surface and 30 km at the standard and significant pressure levels. The standard pressure levels are 1000, 925, 850, 700, 500, 400, 300, 250, 200, 150, 100, 70, 50, 30, 20 and 10 hPa. Significant pressure levels are levels between the standard levels which enable details of the profiles, such as turning points, to be captured. Radiosonde data are also used in the ECMWF and METO assimilation systems.

[13] The GPS-RO/CHAMP temperatures are taken from GeoForschungsZentrum Potsdam (GFZ) version V004 and Jet Propulsion Laboratory (JPL) Level 2 version 1.0 data products, respectively. The SAC-C temperatures are taken from the JPL Level 2 version 1.0 data products. Each satellite observation provides about 200 globally distributed vertical profiles of atmospheric parameters per day within the height interval of 0–50 km. Temperature retrievals are cut off at a much lower altitude because the noise gets so large at altitudes around 40 km. Currently, JPL provides temperature retrievals up to 30 km, and GFZ up to 35 km. In the GFZ and JPL data processor, temperature profiles from the ECMWF and NCEP analysis are used to initialize the hydrostatic equation at 43 km and 30 km, respectively. The derived GPS-RO temperatures depend on the initialization at these altitudes [*Wickert et al.*, 2001a; *Marquardt et al.*, 2003]. The vertical resolution ranges from 0.5 km in the lower troposphere to 1.5 km in the stratosphere and the resolution along the ray path is around a few hundred kilometers. Comparison between vertical profiles of temperature derived by GPS-RO and radiosonde measurements shows no statistically significant differences [*Wickert et al.*, 2004a, 2004b]. The CHAMP and SAC-C JPL profiles occurring within 30 min and 200 km are compared and agree to better than 0.86 K (68% confidence interval) and to within 0.1 K in the mean between 5 and 15 km altitude, after removing the expected variability of the atmosphere [*Hajj et al.*, 2004].

[14] The HALOE temperature data are taken from level 2 version 19 database. The data consist of atmospheric profiles measured by HALOE between ~35 and 77 km, and merged into the NCEP (National Center for Environmental Prediction) data below 34.5 km and the MSIS-86 (Mass Spectrometer Incoherent Scatter) [*Hedin*, 1991] data above 76.5 km. The NCEP data at the lower altitudes was taken for 12:00 GMT time, and may exhibit tidal effects that vary with longitude. The temperatures are retrieved at a 1.5 km vertical spacing and are then interpolated to 0.3 km. Resolution at the higher altitudes throughout the upper stratosphere and the mesosphere is 3 or 4 km. The latitude/longitude location of the HALOE data varies with the spacecraft-Earth-Sun position. For a given day, the locations tend to be in two distinct latitude bands and to sweep across the full longitude range. Coverage across the full range of latitudes between 80°S and 80°N is achieved on a time period ranging from about two to six weeks depending upon the time of year.

[15] An assessment of the quality of HALOE V19 temperature data has been conducted by *Remsberg et al.* [2002] based on comparisons with Rayleigh backscatter lidar and inflatable falling sphere measurements. It is concluded that the HALOE V19 temperatures have little to no bias and that single HALOE profiles are accurate to within their estimated total error (random and systematic) from 37 km to at least 80 km. Random uncertainties for individual profiles are estimated to be $\leq$3 K below 45 km, of the order of 3 to 5 K from 45 to 75 km. Simulated estimates of total bias errors are of the order of 2% (or 5 K).

3. Comparison Methods

[16] The MIPAS and other data sets are searched for coincident measurements. Because of characteristics of the data sampling scenarios, different coincidence criteria have to be applied. As mentioned in the previous section, the ECMWF data are interpolated onto the altitude, latitude, longitude, and UT of the corresponding MIPAS measurements. For MIPAS/METO comparison, the coincidence events are defined by latitude and longitude differences smaller than 1.25° and 1.875°, respectively, i.e., half of the METO data grid, and the time difference less than 1 hour. For comparisons of MIPAS with radiosonde, HALOE, GPS-RO/CHAMP and SAC-C, the horizontal separations between the collocated profiles are required to be smaller than 5° latitude and 10° longitude, but the time differences are 1 hour for radiosonde, 6 hour for GPS-RO/CHAMP and SAC-C, and 12 hours for HALOE. The numbers of correlative profiles used for this study are listed in Table 1. Because of the differences in the data sampling (section 2.2) and the coincidence criteria there are fewer METO coincidences than ECMWF coincidences, and only in 9 and 17 days for the period I and II, respectively.

[17] Table 2 displays the mean spatial separations and temporal differences, as well as their standard deviations, averaged over all available correlative measurements during period I and period II. The mean horizontal distance and time difference between MIPAS and METO correlative measurements are sufficiently small, at ~100 ± 50 km and ~2 ± 30 min. However, for comparisons with CHAMP, SAC-C, HALOE, and RS measurements, the mean horizontal distances are ~500 ± 250 km, and the mean time differences vary between ~0.3 and 3 hours with standard deviations of ~0.5–3 hours. The spatial and temporal mismatches between the correlative measurements are minimized in the polar regions but maximized near the equator (not shown here; see *Wang et al.* [2004c]). This is not surprising since the longitude criterion is meaningless at the poles, and thus the spatial coincidence criteria include only the ±5° in latitude.

[18] The spatial and temporal mismatch can cause temperature differences associated with geophysical variations of the atmospheric field. To quantify the effect of spatial and temporal mismatch, a simulation study has been carried out in a manner similar to that used by *Wang et al.* [2004c]. The METO temperatures at 12:00 UTC for the 14 days in period I are taken as the known atmospheric fields. The

Table 2. Mean Spatial and Temporal Separations and Standard Deviations[a]

	METO	CHAMP (GFZ)	CHAMP (JPL)	SAC-C	HALOE	RS
Distance (period I)	102 ± 46	488 ± 240	446 ± 218	470 ± 224	577 ± 257	515 ± 233
Distance (period II)	101 ± 45	500 ± 244	459 ± 219		439 ± 198	525 ± 233
Latitude (period I)	0.1 ± 0.7	−0.1 ± 2.9	−0.1 ± 2.9	0.0 ± 2.9	0.6 ± 2.8	−0.0 ± 2.9
Latitude (period II)	0.1 ± 0.7	0.0 ± 2.9	0.0 ± 2.9		−0.3 ± 3.0	0.0 ± 2.9
Longitude (period I)	−0.0 ± 1.1	−0.1 ± 5.6	−0.1 ± 5.4	−0.4 ± 5.7	0.6 ± 6.2	0.4 ± 5.6
Longitude (period II)	0.0 ± 1.1	−0.2 ± 5.8	0.1 ± 5.7		−1.1 ± 5.3	−0.2 ± 5.7
Time (period I)	−2 ± 34	161 ± 121	−142 ± 133	−14 ± 142	−116 ± 360	−12 ± 31
Time (period II)	2 ± 35	−134 ± 127	−124 ± 144		−156 ± 393	−5 ± 33

[a]Data are averaged over all available correlative measurements during periods I and II (see Table 1). Horizontal distance is in kilometers, latitude and longitude are in degrees, and time is in minutes.

temperatures at the locations of MIPAS and their correlative measurements are estimated by interpolating the METO data. Their differences and standard deviations are calculated and averaged over the 14 days. The 14-day global mean differences and standard deviations show little height variation, and are thus further averaged over height regions of interest. The estimated overall mean differences and standard deviations are shown in Table 3. The global mean differences are virtually zero for METO and less than 0.2 K for CHAMP, SAC-C, HALOE, and RS, with a tendency for the simulated MIPAS temperatures to be lower than their corresponding measurements. The mean standard deviations are less than 0.5 K for METO, and vary between 1 and 2.6 K for other data sets. These results suggest that imperfect spatial matches have virtually no effect on the observed mean differences since its effect largely averages out but significantly contributes to the observed standard deviations. Note that our estimated standard deviations of 0.5–2.6 K may only provide a low bound for the spatial/temporal mismatch effect, since the simulations do not consider geophysical variations in time and in spatial scales smaller than the METO grids (2.5 degrees in latitude and 3.75 degrees in longitude). More discussions about the effects are presented in section 4.2.

[19] The correlative profiles are interpolated to the altitude grid used by the MIPAS IMK-IAA data processor. Some possible small vertical structures of the temperature field could be resolved by a correlative measurement but not by MIPAS. To account for this effect, the difference δ between the MIPAS profile $\mathbf{x}_{mipas}$ and the correlative profile $\mathbf{x}$ is calculated as

$$\delta = \left(\mathbf{x}_{mipas} - \mathbf{x}\right) + \left(\mathbf{I} - \mathbf{A}_{mipas}\right)\left(\mathbf{x} - \mathbf{x}^{a}_{mipas}\right), \qquad (1)$$

where $\mathbf{I}$ is identity matrix, $\mathbf{A}$ the MIPAS averaging kernel matrix, and $\mathbf{x}^{a}_{mipas}$ is the a priori information used for the MIPAS retrieval. For cases where the altitude resolution of the MIPAS profile and the correlative measurement are substantially different, the effect of a priori information in MIPAS data and its lower-altitude resolution is removed from the difference δ [see also *Wang et al.*, 2004c]. The residuals are taken as proxy for the discrepancy between the two measurements, and assembled in several ways for statistical analysis. For each ensemble, mean difference profiles $\Delta(z)$ and their standard deviations $\sigma(z)$ are calculated. The statistical uncertainty in the mean difference $\Delta(z)$ is quantified by $\sigma(z)/N^{1/2}$, i.e., the 1σ error. This number represents the uncertainty of $\Delta(z)$ due to random-type errors. In the case of $\Delta(z)$ larger than the 1σ error, their difference is an indicator of systematic errors between the comparison data sets, at which this study is targeted. We also compute the mean difference, standard deviation, and 1σ uncertainty averaged over altitude. These height-averaged quantities are directly evaluated according to the statistical definitions by assembling data points available at all height levels.

4. Comparison Results

[20] Detailed profile-by-profile comparisons are performed for the available correlative measurements between MIPAS IMK-IAA temperatures and other data sets (see Table 1). Zonal mean differences are calculated with latitude intervals of 30° and for the MIPAS descending (daytime) and ascending (nighttime) orbit nodes separately. Except for the cases specified otherwise, the results from both nodes are generally similar and thus only daytime results are presented. The global means are averaged over all latitudes and both orbit nodes. The data are averaged over the 14 days of period I and the 20 days of period II separately.

4.1. Comparisons With ECMWF and METO Analyses

[21] The global and zonal mean temperature differences for MIPAS/ECMWF and MIPAS/METO comparisons are displayed in Figures 3 and 4, respectively. Adjustment of vertical resolution and a priori information, described in section 3, is only applied to METO data but not to ECMWF.

[22] In the low to middle stratosphere between 10–30 km, MIPAS temperatures show good agreement with those of

Table 3. Estimated Mean Temperature Differences Δ and Standard Deviations σ Due to Spatial Mismatch Between MIPAS and Correlative Measurements Available in Period I[a]

	METO	CHAMP (GFZ)	CHAMP (JPL)	SAC-C	HALOE	RS
Δ	0.00 ± 0.01	−0.04 ± 0.02	−0.04 ± 0.03	−0.01 ± 0.02	−0.21 ± 0.03	−0.11 ± 0.02
σ	0.44	2.38	2.57	2.21	1.04	1.63

[a]See Table 1. The data are averaged globally over height regions between 10 and 30 km for CHAMP, SAC-C, and RS, between 10 and 50 km for METO, and between 35 and 50 km for HALOE. The statistical uncertainty in the mean difference Δ is quantified by $\sigma/N^{1/2}$, i.e., the 1σ error. Values are in Kelvin.

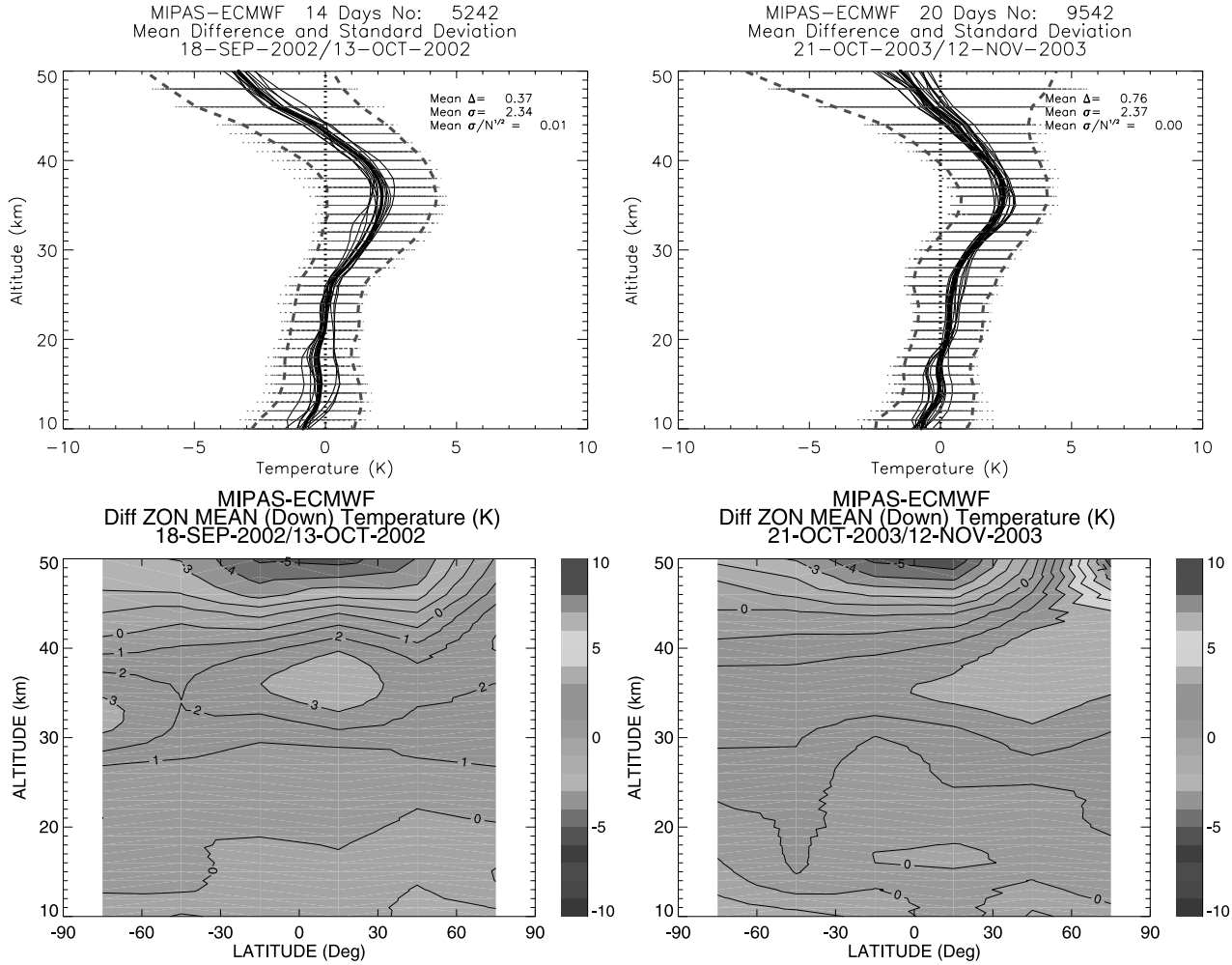

Figure 3. Differences between MIPAS and ECMWF temperatures (in Kelvin). The MIPAS minus ECMWF residuals are calculated from the available correlative measurements (see Table 1). The data are averaged over the (left) 14 days in period I and (right) 20 days in period II. The zonal mean differences are derived with a latitude interval of 30° for the MIPAS descending (daytime, bottom plots) orbit node. The contour intervals are 1 K. On the top plots the global means (solid) and standard deviations (dashed) are computed for each day (thin line) and for all days (thick line) of the observations. The total number of profiles are specified in the headings. Also denoted are the global mean difference Δ, standard deviations σ, and the 1-σ error $\sigma/\sqrt{N}$ averaged over all heights, where N is total number of available data points. See color version of this figure in the HTML.

ECMWF and METO (Figures 3 and 4). The global mean differences for the MIPAS/ECMWF and MIPAS/METO comparisons are less than 0.5–1 K. The standard deviations are estimated as ~1–2 K. The zonal mean differences are less than 1 K in a wide latitude region at the low levels. The discrepancies around 20 km in MIPAS/ECMWF and MIPAS/METO comparisons are smaller in period II than in period I, due to the ILS corrections in the MIPAS retrievals (see section 2.1). Also, between 10 and 27 km MIPAS shows generally better consistency with METO, in comparison with ECMWF, with the global mean differences close to zero at most altitudes in this region. However, it is worth noting that there are discrepancies of ~2 K around 27 km in the global mean differences between MIPAS and METO during period II (Figure 4, top right). These larger biases dominate both polar regions during nighttime (not shown), and are suspected to be a result of problems with the bias correction method used by the METO assimilation system.

[23] Between 30 and 45 km, MIPAS temperatures are generally higher than ECMWF but lower than METO by 2–3 K. The larger discrepancies peak around 35 km and occur around the equator and polar regions in both hemispheres. The systematic MIPAS/METO and MIPAS/ECMWF differences are comparable in amplitude. This feature is thought to be ascribed to a cold bias in the ECMWF and a warm bias in the METO temperatures at these levels. The ECMWF temperatures are known generally to be quite accurate below 10 hPa where bias in the assimilating model is relatively low and both radiosonde and satellite radiance data are assimilated [see, e.g., *Simmons et al.*, 2005], although problems at higher levels

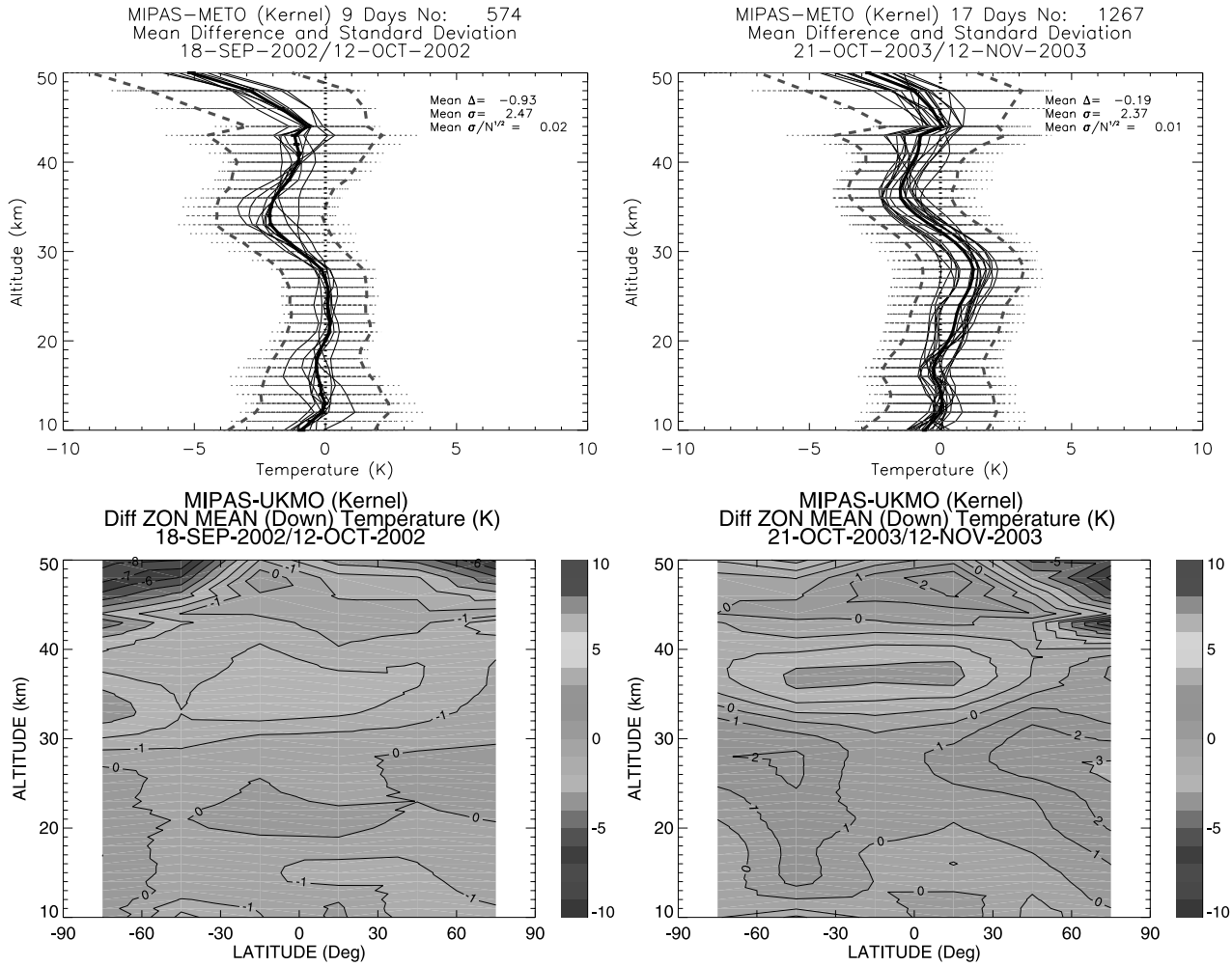

Figure 4. Same as Figure 3, but for comparison between MIPAS and METO temperatures. See color version of this figure in the HTML.

are prone to spread downward below 10 hPa in polar regions, especially in the southern hemisphere. At the higher levels, both ECMWF and METO analyses are essentially derived using AMSU radiance assimilation. In some way it is surprising that they are not more similar. The treatment of radiation, gravity wave drag and the upper boundary condition and limited vertical resolution can contribute to significant model bias, and the absence of radiosonde data makes correction of (generally smaller) biases in the radiance data more problematic than lower down. Recently, *Randel et al.* [2004] compared a number of stratospheric climatologies, including one derived from a few years of the ECMWF ERA-40 reanalysis. The ECMWF reanalysis stood out as the coldest of all data sets between 30 and 45 km. A previous study by *Schöllhammer et al.* [2003a, 2003b] also showed that the largest deviations between ECMWF and METO analyses occurred in the midstratosphere (i.e., 10 hPa, about 30 km) and that the ECMWF data were systematically colder than METO by 5 K, with the root-mean-square (rms) differences peaking at 6 K, and day-to-day differences locally exceeding 10 K.

[24] At the upper levels between 45–50 km, MIPAS is colder than both ECMWF and METO by 2–3 K and 3–5 K, respectively. The discrepancies are reduced in period II in comparison with period I, reflecting the ILS corrections in the MIPAS retrievals (see section 2.1). Referring to the independent comparison between MIPAS and HALOE, which shows that the MIPAS temperatures at 50 km are lower than HALOE temperatures by only 1–2 K, including some tidal influences (see discussions in section 4.4), the large discrepancies of MIPAS/ECMWF and MIPAS/METO comparisons likely suggest deficiencies in the assimilation models at their uppermost levels. In general, the errors will be larger than average at high latitudes and in winter. In particular, errors will be larger (perhaps 10–20 K locally) during dynamically active periods such as stratospheric warmings [*Swinbank and O'Neill*, 1994].

[25] Since the ECMWF analysis is used as a priori information in the IMK-IAA retrievals (see equation (1)), the comparison between $\mathbf{x}_{mipas}$ and $\mathbf{x}^{a}_{mipas} = \mathbf{x}_{ecmwf}$ is meaningful only when the MIPAS retrievals are dominated by MIPAS measurements rather than a priori information, i.e., the diagonal values of $\mathbf{A}_{mipas}$ is reasonably large. Typical matrix $\mathbf{A}_{mipas}$ is dominated by the diagonal elements with values of 0.3–0.5 at the measurement tangent heights [*Wang et al.*, 2004c]. The lowest diagonal values of ~0.2 are seen at the measurement tangent heights below 20 km, where the altitude resolution is worst. Since the constraint in

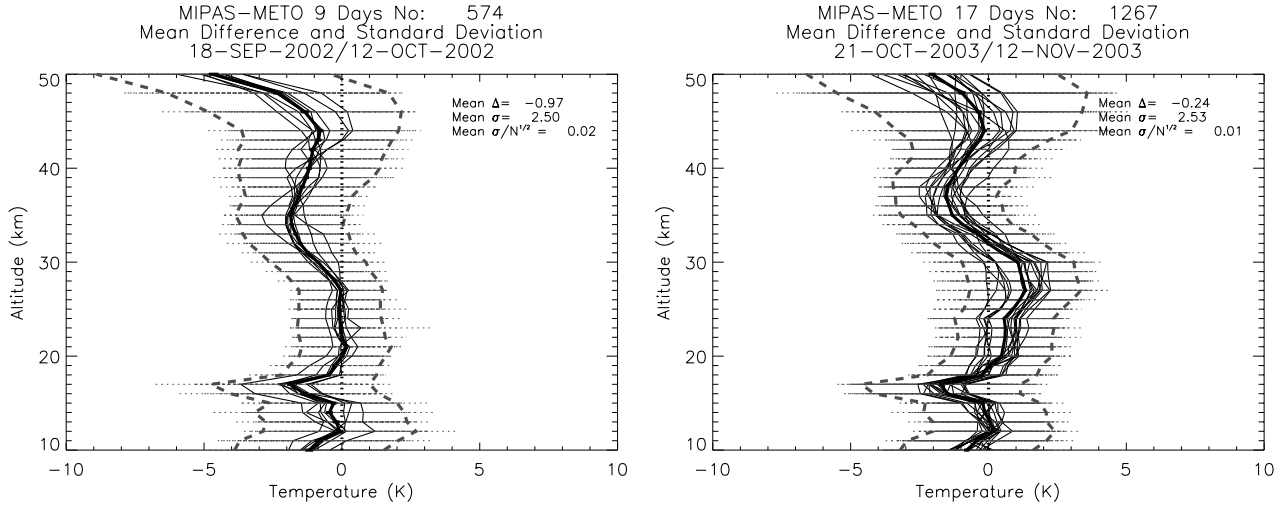

Figure 5. Same as Figure 4, but no adjustment of vertical resolution and a priori is applied to METO data. Also, the zonal mean differences are not shown. See color version of this figure in the HTML.

the MIPAS temperature retrieval is a smoothing constraint rather than a Bayesian one [*von Clarmann et al.*, 2003b], the retrieved profiles are not biased toward the ECMWF profile. This suggests a meaningful comparison between $\mathbf{x}_{mipas}$ and $\mathbf{x}_{ecmwf}$ for all measurement tangent altitudes. Small-scale relative structures of the ECMWF profiles, however, are conserved in the MIPAS retrievals in particular at these low altitudes.

[26] As mentioned above, the METO profiles are adjusted by applying the MIPAS averaging kernel and a priori. This removes the differences originated from different vertical resolution and a priori in the residuals δ in equation (1) (see section 3). To estimate the effect, we take the differences between the MIPAS and METO temperatures, $\mathbf{x}_{mipas} - \mathbf{x}$, i.e., no altitude resolution and a priori adjustment is used, and compute their global mean differences and standard deviations. The results are exhibited in Figure 5. In comparison with the corresponding results for δ (Figure 4, top), significant changes are seen only around 17 km, where the global mean temperatures of MIPAS are lower than those of METO by $\sim$2 K in a narrow height region. The zonal mean differences of $\mathbf{x}_{mipas} - \mathbf{x}$ (not shown here) indicate that MIPAS is colder than METO by as much as $\sim$4 K around the tropopause between 30°S and 30°N, resulting in the -2 K difference in the global means at that altitude. In contrast, these features are not seen in the comparisons between MIPAS and ECMWF (Figure 3).

[27] Two factors could account for the 4 K difference between MIPAS and METO near the tropical tropopause. First, the METO analyses are typically about 1 K warmer than ECMWF in the tropics. Second, but more importantly, the errors of METO analysis could be larger near the tropopause. As shown by *Randel et al.* [2004], ECMWF's ERA-40 analyses were much closer than METO analyses compared to radiosonde data at 100 hPa in the tropics. The sharp temperature minimum is likely not well captured by METO analysis. Given the altitude resolution of the METO data, one should not expect it to do so. However, as discussed above, the MIPAS retrievals calculated at 1 km but with a vertical resolution of $\sim$3 km, must include high-resolution information from the ECMWF a priori profiles. So one should not be surprised if the MIPAS/ECMWF differences are small near the tropopause.

4.2. Comparisons With Radiosonde Data

[28] The IMK-IAA MIPAS temperatures are compared to global radiosonde measurements. Figure 6 displays global and zonal mean temperature differences between the two data sets. Between 10 and 30 km the MIPAS temperatures show good consistencies with the RS data. The global mean differences averaged over all available data points and all height levels are -0.46 ± 0.02 K for period I, and 0.24 ± 0.02 K for period II, with standard deviations of $\sim$2.5 K. The MIPAS temperatures between 10–25 km are generally lower than those of RS in period I but in good agreement in period II because of the ILS corrections in the MIPAS retrievals (see section 2.1). The MIPAS temperatures around 30 km are higher than the RS measurements by $\sim$1–2 K for both observational periods of 2002 and 2003. This is consistent with the comparisons with ECMWF and METO (see Figures 3 and 4), which use the RS data in their assimilation analyses. The zonal mean differences are less than 1 K in a wide latitude region. Large discrepancies of 2–3 K are seen in both polar regions and around the equator, and are thought to be associated with the effects due to the spatial and temporal mismatch between the correlative measurements. The global (Figure 7) and zonal mean (not shown) differences due to the mismatch are nearly zero at most altitudes and latitudes, and the standard deviations are 1–2 K (also see section 3). The largest mean differences of 2 K and standard deviations of 4 K are found between 15 and 30 km in the southern polar regions during period I. The unusual planetary wave activity during the stratospheric major warming and polar vortex split [e.g., *Allen et al.*, 2003], together with increasing spatial/temporal mismatch due to poor radiosonde data control in this region, could be the reasons for the discrepancy.

4.3. Comparisons With GPS-RO CHAMP and SAC-C Observations

[29] The global and zonal mean temperature differences between the MIPAS and GPS-RO retrievals are shown in

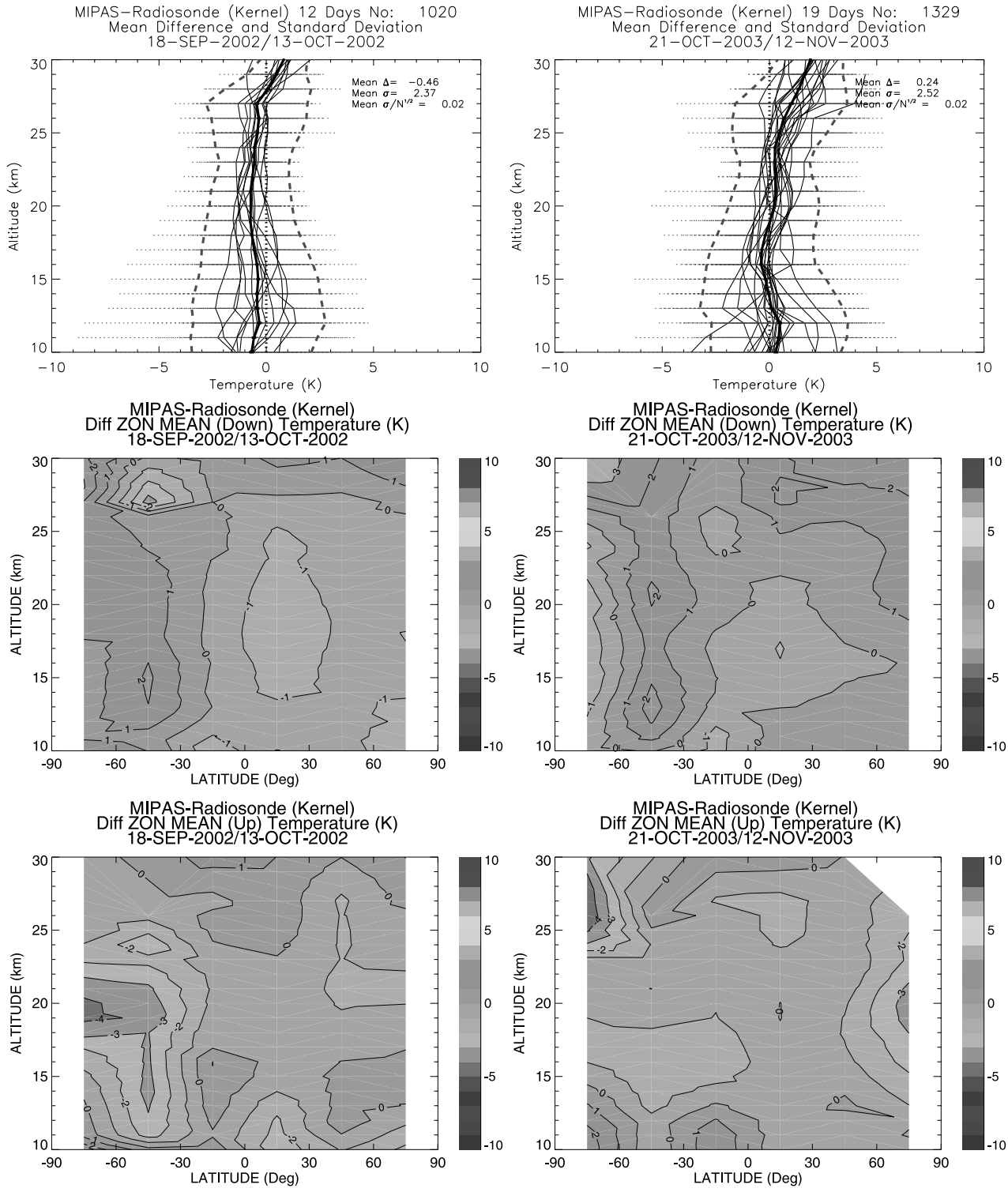

Figure 6. Same as Figure 3, but for comparison between MIPAS and Radiosonde temperatures. Also shown are the zonal mean differences derived for the MIPAS ascending (nighttime, bottom plots) orbit node. See color version of this figure in the HTML.

Figures 8 and 9 for CHAMP GFZ and JPL data during period II, respectively. The CHAMP results for period I are given by *Wang et al.* [2004c]. The comparison with SAC-C measurements of period I was conducted by *Jiang et al.* [2004] without the adjustment of vertical resolution and a priori information, and reanalyzed here with the adjustment applied (Figure 10).

[30] The MIPAS temperatures generally show good consistency with the three GPS-RO data sets. The global mean differences between the MIPAS and individual GPS-RO

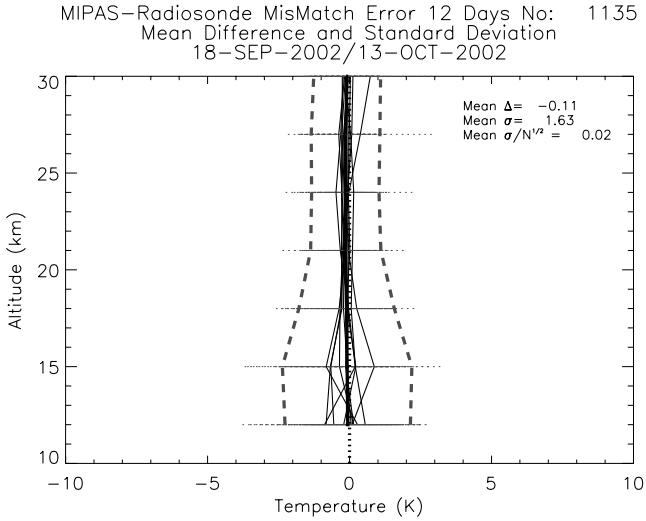

Figure 7. Simulated global mean temperature (in Kelvin) differences (solid) and standard deviations (dashed) due to spatial mismatch between MIPAS and radiosonde correlative measurements during the 14 days of period I (see section 3 for details of the simulation). Denoted are the mean values of $\Delta(z)$, $\sigma(z)$, and $\sigma(z)/N^{1/2}(z)$ averaged over all heights. See color version of this figure in the HTML.

measurements are less than 0.5 K, with standard deviations of ~3 K. The magnitudes of the zonal mean differences are less than 1 K in a wide latitude region. However, large discrepancies of 2–3 K are seen for period I data, in particular in both polar regions and around the equator, while discrepancies of up to 3 K occur around 45°S for period II nighttime data. Also, it is apparent that for daytime measurements and global means, the MIPAS and the three GPS-RO data sets show similar or even better agreement for period II in comparison with period I, probably due to the ILS correction in the MIPAS retrievals (see section 2.1).

[31] Between 10 and 27 km, the MIPAS temperatures tend to be lower than JPL CHAMP and SAC-C data by ~0.5 K but generally consistent with GFZ CHAMP data. Here we should note that the GFZ and JPL data represent "dry" and "wet" temperatures, respectively. The "dry" temperatures derived from GPS-RO measurements could have a cold bias due to the presence of water vapor. In the troposphere around 5 km the difference could be as large as 5 K but decrease above [*Wickert et al.*, 2001b].

[32] The MIPAS temperatures above 27 km are higher than the three GPS-RO data sets. This tendency increases with increasing height and reaches its maximum at 30 km, with magnitudes of ~1 K for the JPL CHAMP and SAC-C data, and ~1.5 K for the GFZ CHAMP data. This is believed to be related to the features of the GPS-RO retrievals. In the GFZ and JPL data processors, temperature profiles from the ECMWF and NCEP analysis are used to initialize the hydrostatic equation at 43 km and 30 km, respectively. The derived GPS-RO temperatures at these altitudes depend on the initialization. If one compares the GFZ or JPL retrievals with the ECMWF or NCEP analyses at 43 km or 30 km, respectively, zero bias and standard deviation (pure ECMWF or NCEP) are expected. This feature is not associated with the measurement principles

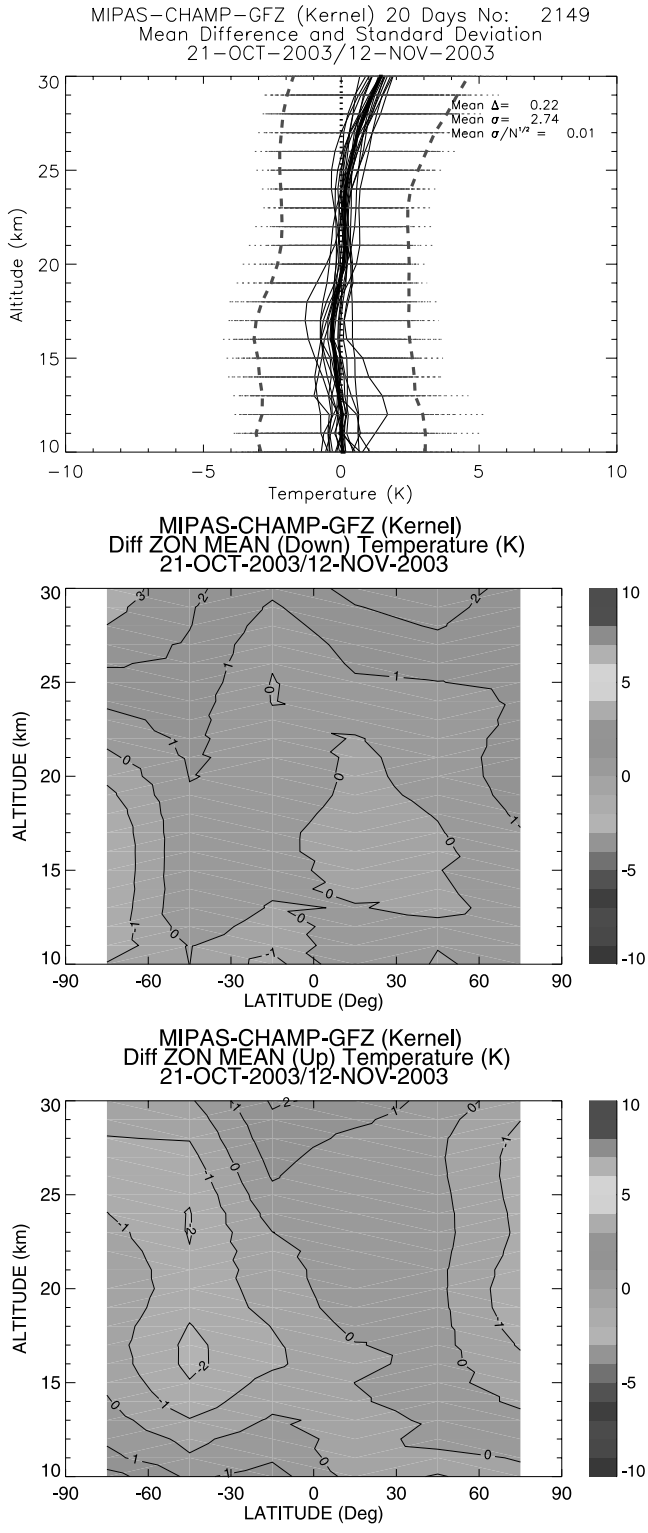

Figure 8. Same as Figure 3, but for comparison between MIPAS and GPS-RO/CHAMP GFZ temperatures in period II. Also shown are the zonal mean differences derived for the MIPAS ascending (nighttime, bottom plot) orbit node. Similar plots for period I are given by *Wang et al.* [2004c]. See color version of this figure in the HTML.

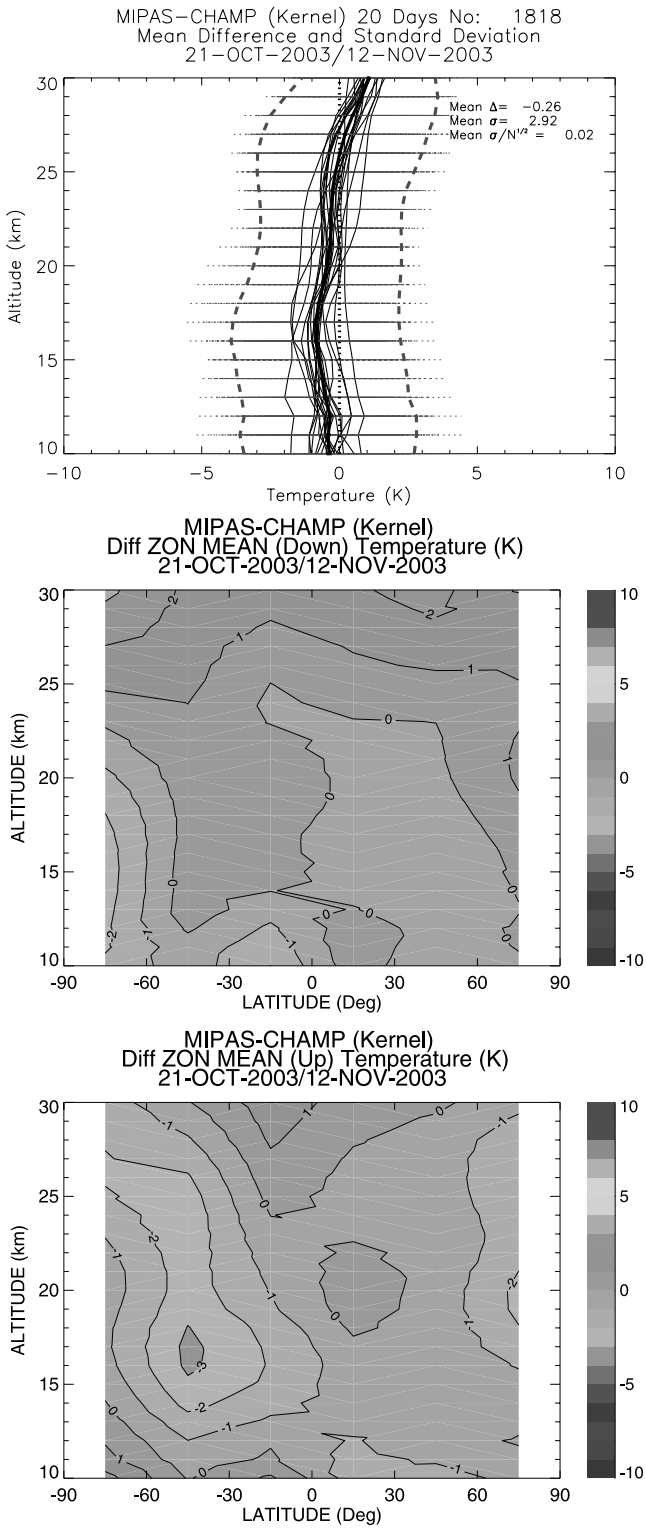

Figure 9. Same as Figure 8, but for comparison between MIPAS and GPS-RO/CHAMP JPL temperatures in period II. Similar plots for period I are given by *Wang et al.* [2004c]. See color version of this figure in the HTML.

but simply due to the very straightforward manner of using the initialization information in the current retrieval scheme. The ECMWF temperatures between 30 and 45 km have a known low bias (see discussions in section 4.1). A comparison has shown that the ECMWF temperatures at 10 hPa (∼30 km) and 20 hPa (∼25 km) for period I are generally lower than NCEP at most latitudes [*Wang et al.*, 2004c]. The cold bias of ECMWF increases with increasing height and reaches a maximum amplitude of ∼2 K. Thus the

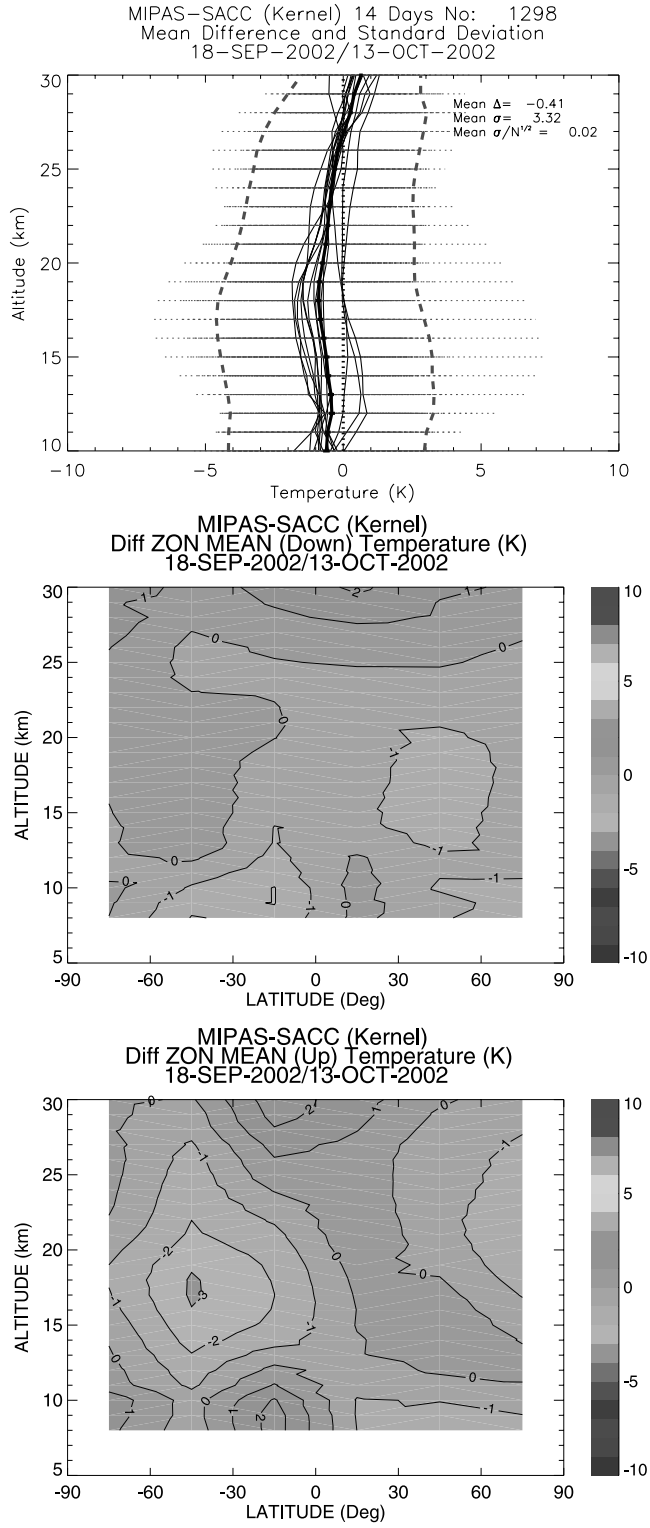

Figure 10. Same as Figure 8, but for comparison between MIPAS and GPS-RO/SAC-C temperatures during period I. See color version of this figure in the HTML.

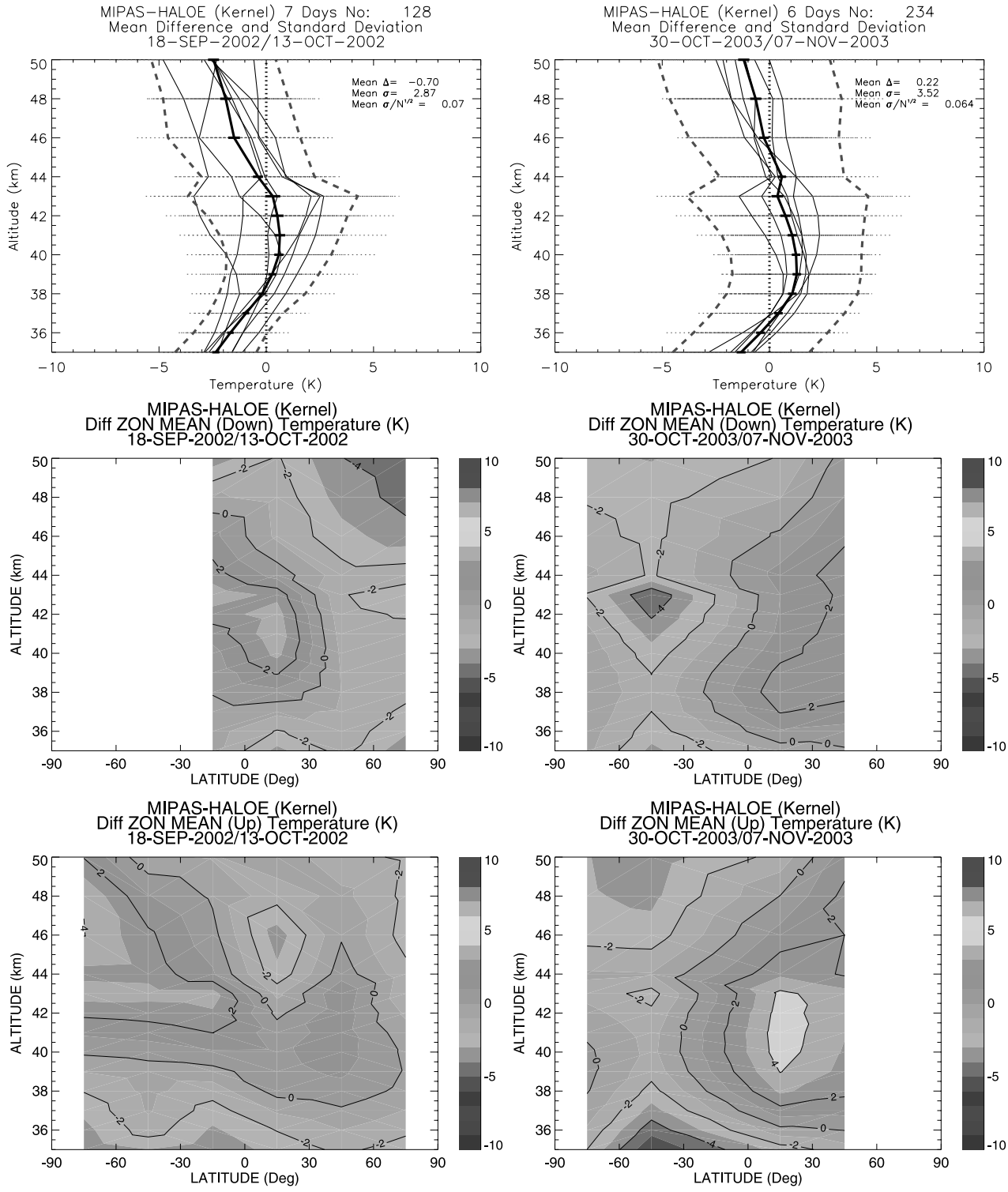

Figure 11. Same as Figure 3, but for comparison between MIPAS and HALOE temperatures. The contour intervals are 2 K. See color version of this figure in the HTML.

deviations between ECMWF and NCEP probably account for the global mean difference at 30 km between GFZ and JPL GPS-RO/CHAMP retrievals.

4.4. Comparisons With HALOE Observations

[33] Figure 11 compares the IMK-IAA MIPAS temperatures with those of HALOE observations between ~35 and 50 km for period I and period II. In these comparisons, the differences in vertical resolution were accounted for by applying the MIPAS averaging kernels. For period I, the MIPAS/HALOE comparisons have been conducted by *Wang et al.* [2004a] without the adjustment of vertical resolution and a priori information and reanalyzed here with the adjustment applied. However, the vertical resolu-

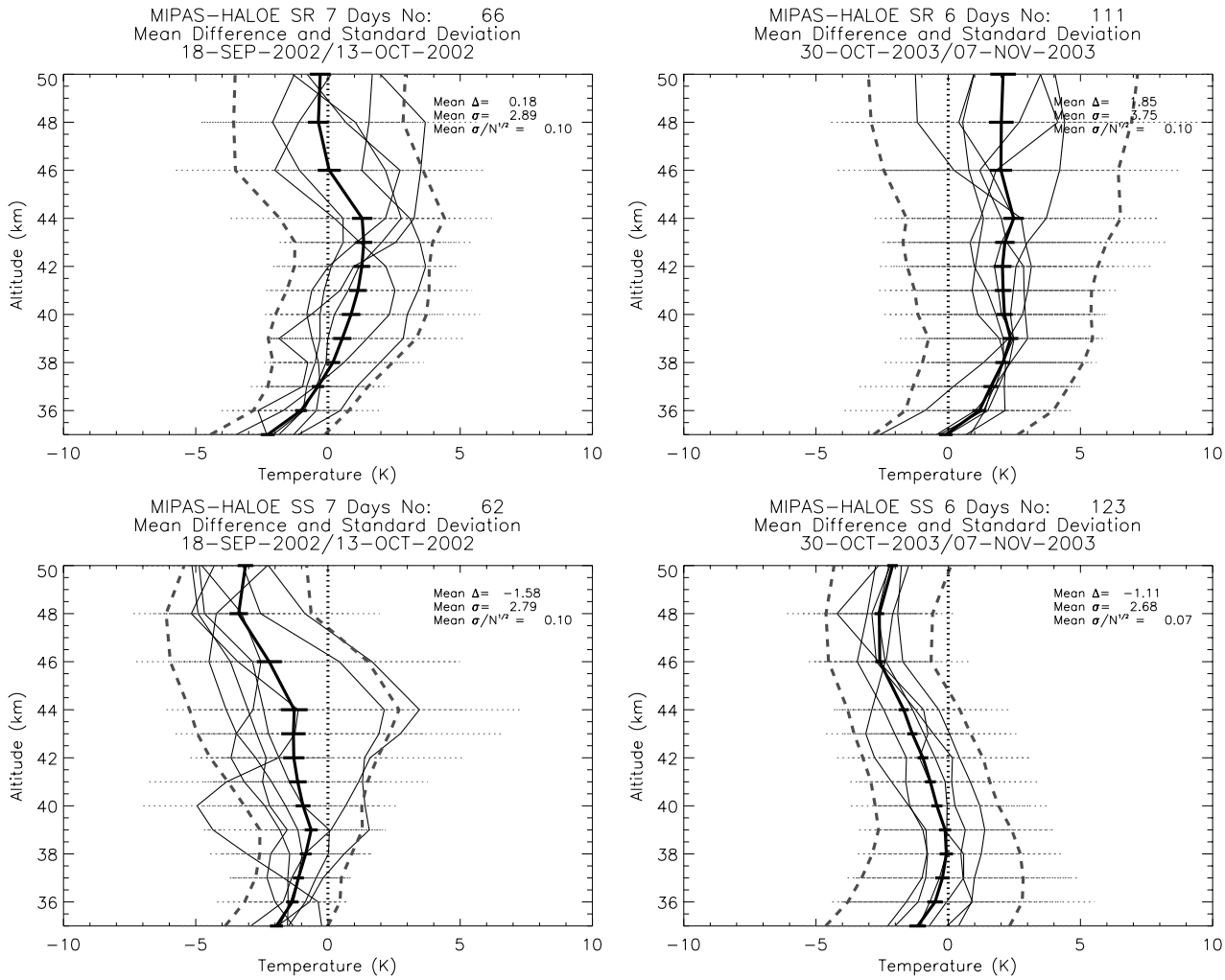

Figure 12. Mean temperature differences (solid) and standard deviations (dashed) (in Kelvin) for the MIPAS/HALOE correlative measurements of (left) September/October 2002 and (right) October/November 2003. The data are averaged for HALOE (top) sunrise and (bottom) sunset events separately. The averages are computed for each day (thin line) and for all days (thick line) of the observations. Also denoted are the global mean difference Δ, standard deviations σ, and the 1σ error $\sigma/\sqrt{N}$ averaged over all heights. See color version of this figure in the HTML.

tion of HALOE is similar to that of MIPAS at altitudes above 36 km, so the convolution should not have made much difference in this region. The MIPAS temperatures show generally good consistency with HALOE, with global mean differences of 1–2 K at individual heights. The IMK-IAA temperatures are higher than HALOE between 38 and 44 km but lower below 38 km and above 45 km. The global mean differences averaged over all heights are -0.70 ± 0.07 K and 0.22 ± 0.06 K for period I and period II, respectively. The discrepancies between MIPAS and HALOE data are reduced in period II with respect to period I. This is thought to be mainly associated with the corrections of ILS information (see section 2.1).

[34] The observed discrepancies between MIPAS and HALOE are thought to be associated at least in part, particularly at low latitudes, with tidal effects which can impart a bias between the correlative pairs if the comparison data are consistently obtained at a different time of the day. This is the case for the MIPAS/HALOE comparison (see the discussion about coincidence criteria in section 3). To quantify the effects, the MIPAS/HALOE correlative measurements are sorted by the HALOE sunset (SS) and sunrise (SR) events. Figure 12 shows the mean differences and standard deviations averaged for the two distinct times. The pattern of the differences for the two events looks different. The MIPAS minus HALOE residuals for the sunrise and sunset events have differences of ±3 K or more. This is in line with the estimates of *Remsberg et al.* [2002]. They examined the sunrise minus sunset differences for an ensemble of 117 March/April pairings for Northern Hemisphere (NH) middle latitudes obtained over a 6-year HALOE period, and found that the tidal amplitudes vary between ±4 K with RMS deviations of 5 K in the altitudes below 50 km. The global mean differences of MIPAS/HALOE comparisons in Figure 11 are calculated by combining the sunrise and sunset cases together. From Figure 12 it is clear that the tidal effects cannot be completely cancelled out when the two cases of limited numbers of data points are combined together.

Table 4. Summary of Mean Differences Δ Between MIPAS and Correlative Temperature Measurements at Different Altitude Regions[a]

	ECMWF	METO	CHAMP (GFZ)	CHAMP (JPL)	SAC-C	HALOE	RS
45–50 km (period I)	−2.6[b]	−3.2[b]				−2.0[b]	
45–50 km (period II)	−0.9	−1.4				−0.7	
30–45 km (period I)	1.4[c]	−1.5[c]				−0.3[c]	
30–45 km (period II)	1.8	−0.7				0.5	
10–30 km (period I)	0.0[d]	−0.2[d]	0.1[e]	−0.4[e]	−0.4[e]		−0.5[e]
10–30 km (period II)	0.2	0.4	0.2	−0.3			0.2

[a]The data are averaged globally in the specified height regions for periods I and II. Values are in Kelvin.

[b]Between 45 and 50 km the largest discrepancies occurred at 50 km, where the mean differences are −3, −5, and −2 in period I and −2, −2, and −1 in period II for ECMWF, METO, and HALOE, respectively.

[c]Between 30 and 45 km the largest discrepancies occurred at 35 km, where the mean differences are +2.5, −2.5, and −2 in period I and −2, −2, and −1 in period II for ECMWF, METO, and HALOE respectively.

[d]Between 10 and 30 km the mean differences are ±1 and ±0.5 K for ECMWF and METO, respectively. However, MIPAS temperatures are higher by 1.5 K around 27 km after introducing the new dynamics in METO assimilation since 29 October 2003.

[e]MIPAS temperatures are higher by 1–1.5 K around 30 km.

[35] We also note possible bias error in the IMK-IAA retrievals due to not accounting for the effects of horizontal path gradients in the temperature field. This error is included in the error budget for the chemical species (assuming temperature gradient of 1 K per 100 km) but currently not for temperature as target. *Steck et al.* [2005] have developed a two-dimensional approach and discussed generally effects of horizontal inhomogeneities on the current one-dimensional MIPAS temperature retrievals. The differences could be significant, up to ±(5–10) K, only in regions where horizontal inhomogeneities are large. This result is in line with that of *Remsberg et al.* [2004], who found such effects to be important, especially near the polar vortex region for the LIMS experiment. The effect of horizontal gradients may contribute to the differences of 2–4 K in the zonal mean plots for 2003 near 50°S, where horizontal gradients of the temperature field are large. Also, it may contribute to the differences for the SS versus SR comparisons, in particular for the 2003 observations (Figure 12, right), for which the SS and SR events occurred around 60°S and 30°N, respectively, with a narrow interval less than 30°.

5. Conclusions

[36] Stratospheric temperatures are retrieved from MIPAS observations using the IMK-IAA data processor. The profiles obtained for September/October 2002 (period I) and October/November 2003 (period II) are compared with several reference data sets, including assimilation analyses of ECMWF and METO, satellite observations of HALOE/UARS, GPS-RO/CHAMP and SAC-C, as well as global radiosonde measurements. The mean differences and standard deviations between MIPAS and the correlative measurements are summarized in Tables 4 and 5, respectively.

[37] Between 10 and 30 km, MIPAS temperatures show good agreement with the six reference data sets. The mean differences averaged over the height interval are within ±0.5 K for comparisons with ECMWF, METO, GPS-RO/CHAMP (both GFZ and JPL data), SAC-C, and RS. The mean differences at individual heights are within ±(1–1.5) K. Between 10 and 25 km, there is a systematic tendency for the MIPAS temperatures to be lower than the JPL data of GPS-RO/CHAMP and SAC-C, but this feature is not seen for the comparisons with the other four data sets. Around 30 km, MIPAS temperatures are higher than ECMWF, RS, and all three GPS-RO data sets by 1–1.5 K, although consistent with METO data assimilated before the new dynamics were introduced on 29 October 2003. Between 30 and 45 km, MIPAS temperatures are higher than ECMWF but lower than METO by 1.5 K for the averages over the height interval, while the mean differences between MIPAS and HALOE data lie between −0.3 and 0.5 K. The larger discrepancies peak around 35 km with magnitudes of ∼2–2.5 K for the three data sets. In the upper stratosphere above 45 km, MIPAS temperatures show a low bias with mean differences of −2, −3, and −5 K compared to HALOE, ECMWF, and METO, correspondingly. The standard deviations of the mean differences show little height variation, and vary between 2.5 and 3.5 K for individual data sets (Table 5).

[38] For the six data sets, the mean differences between 10 and 30 km, either the height averaged values of ±0.5 K or the values of ±(1–1.5) K at individual heights, are within the accuracy of the instrument measurements and assimilation analyses. Even though we do not have access to the error covariances of individual data sets, their accuracy is known to be typically better than 1 K (see discussions for individual comparisons in section 4). The total error for the MIPAS retrievals at stratospheric altitudes is estimated to be 0.3–1.5 K (see section 2.1). This means that near the MIPAS tangent altitudes a total error of 1.2–2.1 K approximately is expected for the differences between correlative profiles. In this perspective, the consistency between the data sets is rather good.

[39] Nonetheless, in the region of 10 and 30 km, a number of comparisons differ more than the expected total error (i.e., the standard deviation of the comparison ensem-

Table 5. Summary of Standard Deviations σ of the Differences Between MIPAS and Correlative Temperature Measurements[a]

	ECMWF	METO	CHAMP (GFZ)	CHAMP (JPL)	SAC-C	HALOE	RS
Period I	2.3	2.5	3.3	3.4	3.3	2.9	2.3
Period II	2.4	2.4	2.7	2.9		3.5	2.5

[a]The data are averaged globally over height regions between 10 and 30 km for CHAMP, SAC-C, and RS, between 10 and 50 km for METO, and between 35 and 50 km for HALOE. Values are in Kelvin.

ble is greater than the expected total error). There are significant temporal and spatial variations of 2–4 K or more in magnitude. Also, large mean differences of 2–4 K or more are observed in the height region between 30 and 50 km. Some features and possible explanations for these observed discrepancies have been examined and noted as follows.

[40] The effect of spatial and temporal mismatch between the correlative measurements contribute little (0.1–0.2 K) to the observed mean differences but significantly (1–2.6 K) to the observed standard deviations for CHAMP, SAC-C, RS, and HALOE (see Table 3). The effects of temporal mismatch are particularly important for HALOE, since the correlative data are consistently obtained at a different time of the day. A bias between the MIPAS minus HALOE residuals for the sunrise and sunset events is ±3 K or more (Figure 12).

[41] Between 30 and 45 km, MIPAS temperatures are generally higher than ECMWF but lower than METO by ~2 K. The larger discrepancies peak around 35 km and occur around the equator and polar regions in both hemispheres. The systematic differences could be, at least by part, explained by deficiency of the models due to lack of observational data control, as discussed in section 4.1. Above 30 km, the assimilation analyses lose radiosonde measurements and model biases become larger. The GPS-RO retrievals need initial temperature setup at the upper level above 30 km. The implementation detail of the initial setup have influence on the GPS-RO retrievals in the mid-stratosphere (see section 4.3).

[42] Different vertical resolutions of the correlative measurements contribute to the observed discrepancies in the tropopause region. The vertical structures of the temperature field near the tropopause could be resolved by the higher-resolution measurements but not by the lower ones. This can introduce ~1 K bias in the observed mean differences between the correlative profiles at that region (see section 4.1 for details).

[43] Finally, the MIPAS IMK data used for this analysis were produced with different versions of level 1B data provided by ESA. Knowledge of the instrumental line shape is insufficient for September/October 2002. This introduced a systematic cold bias of 0.5 K around 20 and 50 km and a weak hot bias of ~0.2 K near 30 km in the MIPAS temperatures of September/October 2002. Thus application of corrected ILS improved the consistency between the MIPAS and other measurements during October/November 2003.

[44] **Acknowledgments.** The British Atmospheric Data Centre (BADC) provided us with access to the Met Office archive of radiosonde, HALOE, and the METO stratospheric assimilation data. Special thanks to Sam Pepler, Anabelle Menochet, and Earl Thompson for preparing radiosonde and HALOE data. ECMWF data obtained from the Envisat validation database, the NILU Atmospheric Database for Interactive Retrieval (NADIR) at Norsk Institutt for Luftforskning (NILU). The research work of IMK-IAA MIPAS group has been funded by EC via contract EVG1-CT-1999-00015 (AMIL2DA), BMBF via project 07 ATF 43/44 (KODYACS), 07 ATF 53 (SACADA), and 01 SF 9953 (HGF-VF), and ESA via contract 15530/01/NL/SF (INFLIC). The IAA team was partially supported by Spanish projects PNE-017/2000-C and REN2001-3249/CLI. B. Funke, M. Kaufmann, and M. E. Koukouli have been supported through an European Community Marie Curie Fellowship. L. Romans and J. H. Jiang acknowledge the support from the Jet Propulsion Laboratory of California Institute of Technology, under contract with NASA.

References

Allen, D. R., R. M. Bevilacqua, G. E. Nedoluha, C. E. Randall, and G. L. Manney (2003), Unusual transport and mixing during the 2002 Antarctic winter, *Geophys. Res. Lett.*, *30*(12), 1599, doi:10.1029/2003GL017117.

Carli, B., et al. (2004), First results of MIPAS/Envisat with operational level 2 code, *Adv. Space Res.*, *33*, 1012–1019.

Dethof, A., A. Geer, W. Lahoz, F. Goutail, A. Bazureau, and D. Wang (2004), MIPAS temperature validation by the MASI group, paper presented at ACVE-2, Eur. Space Res. Inst., Frascati, Italy, 3–8 May.

European Space Agency (2000), Envisat: MIPAS, An instrument for atmospheric chemistry and climate research, *ESA SP-1229*, Noordwijk, Netherlands.

Fischer, H., and H. Oelhaf (1996), Remote sensing of vertical profiles of atmospheric trace constituents with MIPAS limb emission spectrometers, *Appl. Opt.*, *35*(16), 2787–2796.

Hajj, G. A., E. R. Kursinski, L. J. Romans, W. I. Bertiger, and S. S. Leroy (2002), A technical description of atmospheric sounding by GPS occultation, *J. Atmos. Sol. Terr. Phys.*, *64*, 451–469.

Hajj, G. A., C. O. Ao, B. A. Iijima, D. Kuang, E. R. Kursinski, A. J. Mannucci, T. K. Meehan, L. J. Romans, M. de la Torre Juarez, and T. P. Yunck (2004), CHAMP and SAC-C atmospheric occultation results and intercomparisons, *J. Geophys. Res.*, *109*, D06109, doi:10.1029/2003JD003909.

Hedin, A. E. (1991), Extension of the MSIS thermosphere model into the middle and lower atmosphere, *J. Geophys. Res.*, *96*, 1159–1172.

Jiang, J. H., et al. (2004), Comparison of GPS/SAC-C and MIPAS/Envisat temperature profiles and its possible implementation for EOS MLS observations, in *Earth Observation With CHAMP: Results From Three Years in Orbit*, edited by C. Reigber et al., pp. 573–578, Springer, New York.

Marquardt, C., K. Schöllhammer, G. Beyerle, T. Schmidt, J. Wickert, and C. Reigber (2003), Validation and data quality of CHAMP radio occultation data, in *First CHAMP Mission Results for Gravity, Magnetic and Atmospheric Studies*, edited by C. Reigber, H. Lühr, and P. Schwintzer, pp. 384–396, Springer, New York.

Randel, W., et al. (2004), The SPARC intercomparison of middle atmosphere climatologies, *J. Clim.*, *17*, 986–1003.

Remsberg, E., et al. (2002), An assessment of the quality of Halogen Occultation Experiment temperature profiles in the mesosphere based on comparisons with Rayleigh backscatter lidar and inflatable falling sphere measurements, *J. Geophys. Res.*, *107*(D20), 4447, doi:10.1029/2001JD001521.

Remsberg, E. E., L. L. Gordley, B. T. Marshall, R. E. Thompson, J. Burton, P. Bhatt, V. L. Harvey, G. Lingenfelser, and M. Natarajan (2004), The Nimbus 7 LIMS version 6 radiance conditioning and temperature retrieval methods and results, *J. Quant. Spectrosc. Radiat. Transfer*, *86*, 395–424.

Rothman, L. S., et al. (1998), The HITRAN molecular spectroscopic database and HAWKS (HITRAN Atmospheric WorkStation): 1996 edition, *J. Quant. Spectrosc. Radiat. Transfer*, *60*, 665–710.

Russell, J. M., III, L. L. Gordley, J. H. Park, S. R. Drayson, D. H. Hesketh, R. I. Cicerone, A. F. Tuck, J. E. Frederick, J. E. Harries, and P. J. Crutzen (1993), The Halogen Occultation Experiment, *J. Geophys. Res.*, *98*, 10,777–10,797.

Schöllhammer, K., C. Marquardt, and K. Labitzke (2003a), Comparison of three different meteorlogical datasets (ECMWF, Met Office and NCEP), in *First CHAMP Mission Results for Gravity, Magnetic and Atmospheric Studies*, edited by C. Reigber, H. Lühr, and P. Schwintzer, pp. 529–535, Springer, New York.

Schöllhammer, K., C. Marquardt, and K. Labitzke (2003b), Comparision of three different meteorological datasets (ECMWF, MetOffice and NCEP) and CHAMP Temperature Measurements, in *OIST-4 Proceedings, 4th Oersted International Science Team Conference, Copenhagen June 2003*, edited by P. Stauning et al., pp. 255–260, Dan. Meteorol. Inst., Copenhagen.

Simmons, A., M. Hortal, G. Kelly, A. McNally, A. Untch, and S. Uppala (2005), ECMWF analyses and forecasts of stratospheric winter polar vortex break-up: September 2002 in the Southern Hemisphere and related events, *J. Atmos. Sci.*, *62*, 668–689.

Spang, R., J. J. Remedios, and M. P. Barkley (2004), Colour indices for the detection and differentiation of cloud types in infra-red limb emission spectra, *Adv. Space Res.*, *33*(7), 1041–1047.

Steck, T. (2003), Intercomparison of AMIL2DA results for MIPAS-Envisat data, task report, Forschungszentrum Karlsruhe, Karlsruhe, Germany.

Steck, T., M. Höpfner, T. von Clarmann, and U. Grabowski (2005), Tomographic retrieval of atmospheric parameters from infrared limb emission observations, *Appl. Opt.*, in press.

Stiller, G. P., et al. (2003), Early IMK/IAA MIPAS/Envisat results, in *Remote Sensing of Clouds and the Atmosphere VII*, edited by K. Schäfer and O. Lado-Bordowsky, *Proc. SPIE Int. Soc. Opt. Eng.*, *4882*, 184–193.

Swinbank, R., and A. O'Neill (1994), A stratosphere-troposphere data assimilation system, *Mon. Weather Rev.*, *122*, 686–702.

Swinbank, R., N. B. Ingleby, P. M. Boorman, and R. J. Renshaw (2002), A 3D variational data assimilation system for the stratosphere and troposphere, *Forecast. Res. Sci. Pap. 71*, Met Off., Exeter, U. K.

von Clarmann, T., et al. (2003a), A blind test retrieval experiment for limb emission spectrometry, *J. Geophys. Res.*, *108*(D23), 4746, doi:10.1029/2003JD003835.

von Clarmann, T., et al. (2003b), Retrieval of temperature and tangent altitude pointing from limb emission spectra recorded from space by the Michelson interferometer for passive atmosphere (MIPAS), *J. Geophys. Res.*, *108*(D23), 4736, doi:10.1029/2003JD003602.

von Clarmann, T., et al. (2003c), Remote sensing of the middle atmosphere with MIPAS, in *Remote Sensing of Clouds and the Atmosphere VII*, edited by K. Schäfer and O. Lado-Bordowsky, *Proc. SPIE Int. Soc. Opt. Eng.*, *4882*, 172–183.

Wang, D. Y., et al. (2004a), Comparisons of MIPAS-observed temperature profiles with other satellite measurements, in *Remote Sensing of Clouds and the Atmosphere VIII*, edited by K. P. Schäfer et al., *Proc. SPIE Int. Soc. Opt. Eng.*, *5235*, 196–207.

Wang, D. Y., et al. (2004b), Comparisons of MIPAS/Envisat and GPS-RO/CHAMP temperature profiles, in *Earth Observation With CHAMP: Results From Three Years in Orbit*, edited by C. Reigber et al., pp. 567–572, Springer, New York.

Wang, D. Y., et al. (2004c), Cross-validation of MIPAS/ENVISAT and GPS-RO/CHAMP temperature profiles, *J. Geophys. Res.*, *109*, D19311, doi:10.1029/2004JD004963.

Wickert, J., et al. (2001a), Atmosphere sounding by GPS radio occultation: First results from CHAMP, *Geophys. Res. Lett.*, *28*(17), 3263–3266.

Wickert, J., et al. (2001b), GPS ground station data for CHAMP radio occultation measurements, *Phys. Chem. Earth, Part A, Solid Earth Geod.*, *26*, 503–511.

Wickert, J., T. Schmidt, G. Beyerle, R. König, C. Reigber, and N. Jakowski (2004a), The radio occultation experiment aboard CHAMP: Operational data analysis and validation of vertical atmospheric profiles, *J. Meteorol. Soc. Jpn.*, *82*, 381–395.

Wickert, J., T. Schmidt, G. Beyerle, G. Michalak, R. König, J. Kaschenz, and C. Reigber (2004b), Atmospheric profiling with CHAMP: Status of the operational data analysis, validation of the recent data products and future prospects, in *Earth Observation With CHAMP: Results From Three Years in Orbit*, edited by C. Reigber et al., pp. 495–500, Springer, New York.

A. Dethof and A. J. Simmons, European Centre for Medium-Range Weather Forecasts, Shinfield Park, Reading, Berkshire, RG2 9AX, UK.

H. Fischer, N. Glatthor, U. Grabowski, M. Höpfner, S. Kellmann, M. Kiefer, A. Linden, G. Mengistu Tsidu, M. Milz, T. Steck, G. P. Stiller, and T. von Clarmann, Forschungszentrum Karlsruhe GmbH und Universität Karlsruhe, Institut für Meteorologie und Klimaforschung (IMK), Postfach 3640, D-76021 Karlsruhe, Germany.

B. Funke, S. Gil-López, M. E. Koukouli, and M. López-Puertas, Instituto de Astrofísica de Andalucía, CSIC, Apartado Postal 3004, E-18008 Granada, Spain.

J. H. Jiang and L. J. Romans, Jet Propulsion Laboratory, California Institute of Technology, 4800 Oak Grove Drive, Pasadena, CA 91109, USA.

M. Kaufmann, Research Center Juelich (ICG-I), D-52425 Juelich, Germany.

C. Marquardt and R. Swinbank, Met Office, FitzRoy Road, Exeter, EX1 3PB, UK.

E. Remsberg, Atmospheric Sciences Competency, NASA Langley Research Center, Mail Stop 401B, Hampton, VA 23681, USA.

J. Russell III, Department of Physics, Hampton University, Hampton, VA, 23668, USA.

T. Schmidt and J. Wickert, Department 1, Geodesy and Remote Sensing, GeoForschungsZentrum Potsdam (GFZ), Telegrafenberg, D-14473 Potsdam, Germany.

D. Y. Wang, Science Application International Corporation/General Science Operation, MODIS Characterization Support Team, 7501 Forbes Boulevard, Suite 103, Seabrook, MD 20706, USA. (ding.yi.wang@saicmodis.com)